

Chapter III. STATUS OF EXISTING NEUTRON EDM MEASUREMENTS

The history of neutron EDM measurements is closely interwoven with our evolving knowledge of discrete symmetries in physics. In 1950, when parity was considered an inviolable symmetry, Purcell and Ramsey [1] pointed out the need to test this symmetry via detection of a neutron EDM. They then carried out a pioneering experiment [2,3] setting an upper limit at 5×10^{-20} e-cm for neutron EDM. The role of the baryon (proton, neutron, hyperons) EDM in testing parity symmetry was extensively discussed in the seminal paper of Lee and Yang [4], who cited the yet-unpublished neutron EDM result from Smith, Purcell, and Ramsey [2,5].

The discovery of parity violation in 1957 [6–8] prompted Smith et al. to publish their neutron EDM result [3]. By this time, however, it was recognized [9,10] that time-reversal invariance would also prevent the neutron from possessing a non-zero EDM. Since no evidence of T violation was found even in systems that exhibited maximal parity violation, a non-zero neutron EDM was regarded as highly unlikely. However, Ramsey [10a] emphasized the need to check time-reversal invariance experimentally. He also pointed out that Dirac's magnetic monopole violates both P and T symmetry. The experimental activities on the neutron EDM lay dormant until CP violation, directly linked to T violation via the CPT theorem [11–13], was discovered in 1964 [14].

The interest in the neutron EDM was greatly revived when a large number of theoretical models, designed to account for the CP-violation phenomenon in neutral kaon decays, predicted a neutron EDM large enough to be detected. Many ingenious technical innovations have since been implemented, and the experimental limit of neutron EDM was pushed down to 10^{-25} e-cm, a six order-of-magnitude improvement over the first EDM experiment. Unlike parity violation, the underlying physics for CP and T violation remains a great enigma nearly 40 years after its discovery. As discussed in Chapter II, improved neutron EDM measurements will continue to provide the most stringent tests for various theoretical models and to reveal the true origins of CP violation.

Table III-A lists the results from all existing neutron EDM experiments. In Fig. III-1 the neutron EDM upper limits are plotted versus year of publication. The different symbols in Fig. III-1 signify different experimental techniques. The experimental techniques fall into three categories. Category I, which consists of only two experiments, utilizes neutron scattering to probe the effect of the neutron EDM. The strong electric fields encountered by polarized neutrons in scattering from electrons or nuclei, could affect the

Table III-A. Summary of Neutron EDM experiments.

| Ex. Type (Lab) | $\langle v \rangle$ (m/sec) | E (kV/cm) | B (Gauss) | Coh. Time (sec) | EDM ($e \cdot \text{cm}$) | Ref. (year) |
|-------------------------------|--------------------------------|----------------|----------------|--------------------|--|------------------|
| Scattering (ANL) | 2200 | $\sim 10^{15}$ | — | $\sim 10^{-20}$ | $< 3 \times 10^{-18}$ | [1,16] (1950) |
| Beam Mag. Res. (ORNL) | 2050 | 71.6 | 150 | 0.00077 | $(-0.1 \pm 2.4) \times 10^{-20}$ $< 4 \times 10^{-20}$ (90% C.L.) | [3] (1957) |
| Beam Mag. Res. (ORNL) | 60 | 140 | 9 | 0.014 | $(-2 \pm 3) \times 10^{-22}$ $< 7 \times 10^{-22}$ (90% C.L.) | [22] (1967) |
| Bragg Reflection (MIT/BNL) | 2200 | $\sim 10^9$ | — | $\sim 10^{-7}$ | $(2.4 \pm 3.9) \times 10^{-22}$ $< 8 \times 10^{-22}$ (90% C.L.) | [17] (1967) |
| Beam Mag. Res. (ORNL) | 130 | 140 | 9 | 0.00625 | $(-0.3 \pm 0.8) \times 10^{-22}$ $< 3 \times 10^{-22}$ | [23] (1968) |
| Beam Mag. Res. (BNL) | 2200 | 50 | 1.5 | 0.0009 | $< 1 \times 10^{-21}$ | [26] (1969) |
| Beam Mag. Res. (ORNL) | 115 | 120 | 17 | 0.015 | $(1.54 \pm 1.12) \times 10^{-23}$ $< 5 \times 10^{-23}$ | [24] (1969) |
| Beam Mag. Res. (ORNL) | 154 | 120 | 14 | 0.012 | $(3.2 \pm 7.5) \times 10^{-24}$ $< 1 \times 10^{-23}$ (80% C.L.) | [25] (1973) |
| Beam Mag. Res. (ILL) | 154 | 100 | 17 | 0.0125 | $(0.4 \pm 1.5) \times 10^{-24}$ $< 3 \times 10^{-24}$ (90% C.L.) | [28] (1977) |
| UCN Mag. Res. (PNPI) | • 6.9 | 25 | 0.028 | 5 | $(0.4 \pm 0.75) \times 10^{-24}$ $< 1.6 \times 10^{-24}$ (90% C.L.) | [31] (1980) |
| UCN Mag. Res. (PNPI) | • 6.9 | 20 | 0.025 | 5 | $(2.1 \pm 2.4) \times 10^{-25}$ $< 6 \times 10^{-25}$ (90% C.L.) | [32] (1981) |
| UCN Mag. Res. (ILL) | • 6.9 | 10 | 0.01 | 60–80 | $(0.3 \pm 4.8) \times 10^{-25}$ $< 8 \times 10^{-25}$ (90% C.L.) | [36] (1984) |
| UCN Mag. Res. (PNPI) | • 6.9 | 12–15 | 0.025 | 50–55 | $-(1.4 \pm 0.6) \times 10^{-25}$ $< 2.6 \times 10^{-25}$ (95% C.L.) | [35] (1986) |
| UCN Mag. Res. (ILL) | • 6.9 | 16 | 0.01 | 70 | $-(3 \pm 5) \times 10^{-26}$ $< 12 \times 10^{-26}$ (95% C.L.) | [41] (1990) |
| UCN Mag. Res. (PNPI) | • 6.9 | 12–15 | 0.018 | 70–100 | $(2.6 \pm 4.5) \times 10^{-26}$ $< 9.7 \times 10^{-26}$ (90% C.L.) | [38] (1992) |
| UCN Mag. Res. (ILL) | • 6.9 | 4.5 | 0.01 | 120–150 | $(-1 \pm 3.6) \times 10^{-26}$ $< 6.3 \times 10^{-26}$ (90% C.L.) | [47] (1999) |

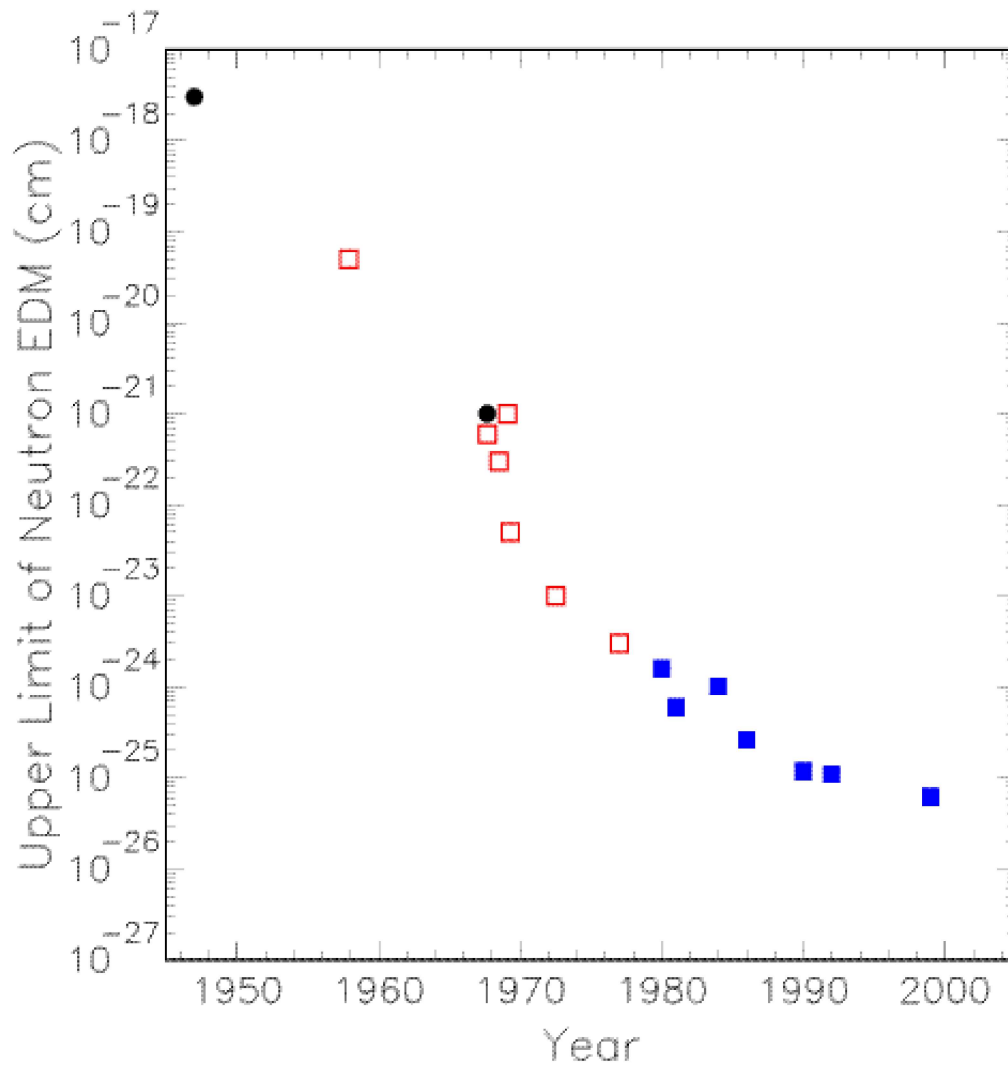


Fig. III-1. Upper limits of neutron EDM plotted as a function of year of publication. The solid circles correspond to neutron scattering experiments. The open squares represent in-flight magnetic resonance measurements, and the solid squares signify UCN magnetic resonance experiments.

scattering amplitudes if the neutron has a non-zero EDM. The second and third categories both involve magnetic resonance techniques. In the presence of a strong external electric field, a finite neutron EDM would cause a shift of the magnetic resonance frequency. From 1950 to mid 1970s, thermal or cold neutron beams have been used in the measurements (category II). Since early 1980s, all neutron EDM experiments have utilized bottled UCNs (category III), which provide the most sensitive measurements to date.

A) Neutron EDM from Neutron Scattering

The upper limit of the neutron EDM was first determined in 1950 by Purcell and Ramsey [1] from an analysis of earlier experiments of neutron-nucleus scattering [15,16]. In these experiments, the strength of the neutron-electron interaction was deduced from the interference between the neutron-nucleus and neutron-electron scattering. If the observed neutron-electron interaction strength is attributed entirely to the neutron EDM (d_n), an upper limit of $\bar{d}_n \leq 3 \times 10^{-18} e\cdot\text{cm}$ is obtained.

An alternative method to extract the electron-neutron interaction is to scatter electron beam from nuclear targets. Indeed, precise $e-d$ and $e\text{-}^3\text{He}$ scattering data have been obtained at various electron accelerators. However, we are not aware of any attempt to extract upper limits of neutron EDM based on these data. Since the electron-neutron interaction is dominated by the electric and magnetic form factors of the neutron, any effect due to neutron EDM is probably too small to be observed.

Another technique to search for the neutron EDM is the Bragg reflection of thermal neutrons from a single crystal. The scattering amplitude of thermal neutrons comes mainly from the nuclear interaction. However, the Coulomb field exerted by the positively charged nucleus on the incident neutron can provide additional contributions. First, it produces an effective magnetic field of $\bar{v} \times \bar{E}$ in the neutron rest frame. The neutron magnetic moment interacts with this magnetic field (Schwinger scattering) leading to the following contribution to the scattering amplitude:

$$\begin{aligned} f_{\text{Sch}} &= i f'_{\text{Sch}}, \\ f'_{\text{Sch}} &= \frac{1}{2} \mu_n (\hbar/Mc) (Ze^2/\hbar c) (1-f) \cot \theta \bar{P} \cdot \bar{n}, \end{aligned} \quad (\text{III.1})$$

where \bar{P} is the polarization vector of the neutron, \bar{n} is the unit vector normal to the neutron scattering plane, and θ is the neutron scattering angle. μ_n is the neutron magnetic moment and f is the electron screening factor. The Schwinger scattering amplitude is purely imaginary and is proportional to $\bar{P} \cdot \bar{n}$. The effect of Schwinger scattering is maximal when the neutron polarization is perpendicular to the scattering plane. If the neutron polarization lies in the scattering plane, then $f_{\text{Sch}} = 0$.

If the neutron has a non-zero EDM, the Coulomb field of the nucleus would lead to an additional potential $V_d(\mathbf{r}) = -\vec{d}_n \cdot \vec{E}(\mathbf{r})$, where \vec{d}_n is the neutron EDM. The scattering amplitude contributed by this interaction is

$$\begin{aligned} f_d &= if'_d, \\ f'_d &= \frac{Ze(1-f)}{\hbar v} d_n \csc \theta \vec{P} \cdot \vec{e}, \end{aligned} \quad (\text{III.2})$$

where $\vec{e} = (\vec{k}' - \vec{k})/2k \sin \theta$. \vec{k} and \vec{k}' are the wave vectors for the incident and scattered neutron, respectively. Similar to the Schwinger scattering, the neutron EDM interaction also gives rise to an imaginary scattering amplitude. However, f_d is maximal when the neutron polarization vector \vec{P} lies on the scattering plane and is aligned with \vec{e} (note that $f_{\text{Sch}} = 0$ in this case). This is an important feature that allows the isolation of the f_d contribution.

In measurements at MIT and BNL, Shull and Nathans [17] attempted to determine the f_d term by measuring Bragg reflection of polarized neutrons off a CdS crystal. If the neutron polarization is in the plane of scattering, then f_{Sch} does not contribute and the Bragg reflection intensity I is given as

$$I \sim F^2 V \sim \left[a^2 + (a' - f'_d)^2 \right] V, \quad (\text{III.3})$$

where a and a' are the real and imaginary parts of the nuclear scattering length, respectively. F is the crystal structure factor and V is the effective volume of the crystal. Upon a reversal of the polarization direction of the neutron beam, f'_d flips sign and the fractional change in the intensity becomes

$$\Delta I/I = 4a'f'_d / (a^2 + a'^2). \quad (\text{III.4})$$

Equation (III.4) shows that it is important to find a crystal with a large value of a'/a . In general, however, the value of a'/a is very small. In a few special cases, when there is a resonance absorption cross section of the order of 10^4 barns, $a'/a \simeq 1$. In particular, a cadmium crystal has $a = 0.37 \times 10^{-12}$ cm and $a' = 0.6 \times 10^{-12}$ cm. Shull and Nathans selected the CdS crystal for their Bragg reflection measurement, because at the [004] orientation of the crystal, $a = a_{\text{Cd}} - a_{\text{S}}$, and the real part of the scattering length from S largely cancels that from Cd ($a_{\text{S}} = 0.28 \times 10^{-12}$ cm and a'_{S} is negligible). Following a three-month run with 4×10^8 neutrons counted, they obtained [17] an upper limit for the neutron EDM as 5×10^{-22} e-cm.

An important limitation of the crystal reflection method is the difficulty to align the crystal orientation (hence the scattering plane) with the polarization direction of the incident neutrons. Any residual misalignment would allow the Schwinger scattering to contribute to ΔI in a fashion similar to neutron EDM. A rotation of the crystal-detector assembly by 180° around an axis in the beam direction in principle can isolate the effect of Schwinger scattering, provided that there is no residual magnetic field which does not rotate with the apparatus (such as earth's magnetic field). The limit on d_n of the Shull and Nathans experiment is consistent with a misalignment angle of 1.6 ± 1.0 mrad.

It is likely that the Bragg reflection technique can be further refined to achieve better sensitivity. In particular, Alexandrov et al. [18] suggested that a crystal made of tungsten isotopes enriched with ^{186}W has several advantages over the CdS crystal. First, tungsten has a higher Z than cadmium, leading to a twofold gain in f_d . Second, the real part of the scattering length of the tungsten crystal can be made practically zero by fine-tuning the ^{186}W concentration. As shown in Eq. (III.4), this leads to a larger effect in ΔI . Third, the imaginary part of the scattering length of tungsten is roughly a factor of 150 smaller than that of CdS. This implies a much larger effective volume V for tungsten, since the penetration depth L of the Bragg reflection is proportional to $(a^2 + a'^2)^{-1/2}$. Putting together all these factors, it was estimated that the running time could be reduced by a

factor of 500 to achieve the same statistical accuracy as obtained in the CdS experiment. However, such improvement is not sufficient to make it competitive with respect to the magnetic resonance method, to be described in the next subsection.

Another type of crystal diffraction experiment has been suggested which can increase the effective neutron interaction time by a factor of ~ 100 . It requires neutrons incident at the Bragg angle on a large perfect crystal oriented in the Laue arrangement. Neutrons will experience multiple Bragg reflections resulting in a wave traveling along the Bragg planes. The intensity of the transmitted neutrons will exhibit an oscillatory pattern along a direction perpendicular to the Bragg planes. Such interference fringes, called Pendellösung (Pendulum) by Ewald in his study of X-ray diffraction, were first observed for neutron beams by Shull [19]. Since the location of the fringe is highly sensitive to the neutron scattering amplitude, a non-zero neutron EDM would generate a shift of the fringe pattern, provided that a non-centrosymmetric crystal (such as BGO) is used. If one selects nuclei with low neutron absorption, a large crystal (several centimeters thick) would allow neutrons to be transmitted with little loss. This corresponds to an observation time of $\sim 10^{-5}$ seconds which is 100 times longer than for the Bragg reflection method. The expected statistical sensitivity has been estimated to be around 3×10^{-25} e-cm per day, very competitive to any other technique. Unfortunately, the crystal needs to be aligned to an accuracy of 10^{-7} radian, a difficult if not insurmountable problem.

B) Neutron EDM from In-Flight Neutron Magnetic Resonance

The method used in this type of measurement is similar to the magnetic resonance technique invented by Alvarez and Bloch [20] for a neutron magnetic moment measurement. Essentially, transversely polarized neutrons traverse a region of fixed uniform magnetic field \vec{B}_0 and a static electric field \vec{E}_0 parallel to \vec{B}_0 . The neutrons precess at the frequency

$$h\nu = -2\mu B_0 - 2d_n E_0 , \quad (\text{III.5})$$

where μ is the neutron magnetic dipole moment and d_n is the neutron EDM. Upon reversal of the electric field direction, the precession frequency will shift by

$$h\Delta\nu = -4d_nE_0 . \quad (\text{III.6})$$

Therefore, by measuring the precession frequency with the electric field parallel and antiparallel to the magnetic field, the neutron EDM can be determined as

$$d_n = \frac{h\Delta\nu}{4E_0} . \quad (\text{III.7})$$

The neutron precession frequency can be accurately measured using the technique of separated oscillatory fields developed by Ramsey [21]. Oscillating magnetic fields of identical frequency are introduced at each end of the homogeneous-field region. Spin-flip transitions are induced in the neutron beam when the frequency of the applied oscillatory magnetic field approaches the neutron precession frequency. The fraction of neutrons emerging from the spectrometer with their spins flipped depends sensitively on the frequency of the oscillating field. The goal of the neutron EDM experiment is to accurately determine the shift of the resonance frequency when the direction of the electric field is reversed.

Following the pioneering work of Purcell et al. at Oak Ridge in 1950, various improvements of the experimental techniques have been introduced and similar experiments were carried out at Oak Ridge [22–25], Brookhaven [26], Bucharest [27], Aldermaston, and Grenoble [28]. Table III-A lists some characteristics of these experiments. The 1977 measurement [28] at the Institut Laue-Langevin (ILL), Grenoble represented a four order-of-magnitude improvement in sensitivity over the original Oak Ridge experiment. This was accomplished by minimizing the statistical and systematic errors. We will now discuss the factors contributing to the statistical and systematic errors for this type of experiment.

Equation (III.7) shows that d_n is proportional to $\Delta\nu$, given as

$$\Delta\nu = \Delta N / (dN / d\nu) , \quad (\text{III.8})$$

where N is the number of neutron counts per cycle and $dN / d\nu$ is the slope of the resonance curve. To achieve maximal sensitivity, the oscillator frequency is set near the steepest slope of $dN / d\nu$. In this case, $(dN / d\nu) / N$ is proportional to the neutron time-

of-flight between the two RF coils and to the neutron polarization P . The flight time is simply $L/\langle v \rangle$, where L is the distance between the RF coils and $\langle v \rangle$ is the mean neutron velocity. ΔN is proportional to $(\phi_n t)^{1/2}$, where ϕ_n is the flux of neutrons and t is the total running time. Taking these factors into account, one obtains the following relation for the statistical uncertainty in d_n :

$$\Delta d_n \propto \langle v \rangle / [E_0 L P (\phi_n t)^{1/2}] . \quad (\text{III.9})$$

To obtain maximal sensitivity, the experiment needs to maximize the electric field E_0 , the distance L , the neutron polarization P , and the neutron flux ϕ_n . In addition, the mean neutron velocity $\langle v \rangle$ needs to be minimized. Table III-A lists these parameters for various experiments.

Many sources of systematic errors have been identified and the dominant ones are:

- The $\bar{v} \times \bar{E}$ effect.
- Fluctuation of the magnetic field.

The $\bar{v} \times \bar{E}$ effect, also called the motional field effect, refers to the additional magnetic field \bar{B}_m viewed from the neutron rest frame,

$$\bar{B}_m = \frac{1}{c} \bar{v} \times \bar{E}_0 , \quad (\text{III.10})$$

where \bar{v} is the neutron velocity in the lab frame. If the electric field \bar{E}_0 is not completely aligned with the magnetic field \bar{B}_0 , then \bar{B}_m would acquire a non-zero component along the direction of \bar{B}_0 . Upon reversal of the electric field direction, this component will also reverse direction and produce the same signature as would a neutron EDM. An apparent EDM resulting from the motional field effect is

$$d_n = [(\mu_n / \mu_N) / 4\pi] \lambda_c (v/c) \sin \theta , \quad (\text{III.11})$$

where μ_N is the nuclear magneton, θ is the angle between the B and E fields, and λ_c is the Compton wavelength of the proton. Equation (III.11) shows that for a cold neutron of 100 m/sec, a misalignment angle of 1.5×10^{-3} radians would lead to an apparent neutron EDM of 10^{-23} e·cm.

Careful attention has been given to alignment of the B and E fields. A tight geometric tolerance was imposed to make the magnetic pole faces parallel to the electric plates. In

one experiment [26], the magnetic pole faces also serve as the electric field electrodes. Stray ambient magnetic fields could also contain components perpendicular to the E field, and the spectrometer needs to be surrounded by several magnetic shields. By rotating the entire spectrometer by 180° around a vertical axis, the $\vec{v} \times \vec{E}$ effect can be isolated.

The applied magnetic field needs to be spatially homogeneous and temporally stable. Since neutrons follow different paths in the spectrometer, any spatial non-uniformity would degrade the sharpness of the resonance. The temporal stability is even more critical. In particular, any systematic variation of the magnetic field correlated with the reversal of electric field must be minimized. It can be shown that in order to achieve a sensitivity of $10^{-24} e\cdot\text{cm}$ for d_n , the allowable magnetic noise correlated with the electric field reversal must be below a few nano Gauss. A shift of the magnetic field can be caused, for example, by the breakdowns in the electric field. The current pulse associated with the spark could permanently magnetize small portions of the pole faces, and the direction of such magnetic field is correlated with the polarity of the electric field. Another type of spurious magnetic field correlated with the electric field is the leakage current. Fortunately, for neutron beam experiments, the bulk of the leakage current occurs outside the spectrometer and does not pose a problem.

As shown in Table III-A, the most sensitive neutron beam (Category II) experiment [28], obtained:

$$d_n = (0.4 \pm 1.5) \times 10^{-24} e \cdot \text{cm} , \quad (\text{III.12})$$

where the total error contains a systematic error of $1.1 \times 10^{-24} e\cdot\text{cm}$. The dominant contribution to the systematic error is the $\vec{v} \times \vec{E}$ effect, even though the misalignment angle is determined to be as small as 1.1×10^{-4} radians. The limitations from $\vec{v} \times \vec{E}$ effect and from the magnetic field fluctuation can be removed by using bottled UCN, to be discussed next.

C) Neutron EDM with Ultra-Cold Neutrons

There are two major limitations in the search for neutron EDM using thermal or cold neutron beams. First, the $\vec{v} \times \vec{E}$ effect imposes stringent requirements on the alignment of the \vec{E} and \vec{B} fields, as discussed earlier. Second, the transit time of neutron beams in the magnetic spectrometer is relatively short, being 10^{-2} seconds roughly. This leads to a

rather large width of the resonance curve and implies the necessity to measure very small variations of the neutron counts. Therefore, any systematic effects associated with the reversal of the electric field would have to be reduced to extremely low levels. These and other limitations are responsible for the fact that the best upper limit for neutron EDM achieved with the cold neutron beam at ILL is $3 \times 10^{-24} e \cdot \text{cm}$ even though the statistical uncertainty is at a lower level of $\sim 3 \times 10^{-25} e \cdot \text{cm}$.

In 1968 Shapiro first proposed [29] using UCN in searches for neutron EDM. The much lower velocities of UCNs will clearly suppress the $\vec{v} \times \vec{E}$ effect. The amount of suppression is further enhanced in an UCN bottle, which allows randomization of the neutron momentum directions. Another important advantage is that the effective interaction time of UCN in a storage bottle will be of the order $10^2 - 10^3$ seconds, a factor of $10^4 - 10^5$ improvement over the neutron beam experiments. This significantly improves the sensitivity for EDM signals relative to EDM-mimicking systematic effects. An important price to pay, however, is the much lower flux for UCN relative to that of thermal or cold neutron beams.

A series of neutron EDM experiments using UCN has been carried out at the Petersburg Nuclear Physics Institute (PNPI) and at the ILL. Although there are many similarities in the approaches of these two groups, important differences do exist. In the following, we summarize the pertinent features and results of these experiments.

C.1) UCN Measurements at PNPI

Immediately following Shapiro's original proposal [29], preparation for an UCN neutron EDM experiment started at PNPI in 1968. The first version of the experiment, reported in 1975 [30], used a single-chamber "flow-through" type spectrometer with separated oscillating fields. An uncooled beryllium converter provided low flux of UCN and the width of the magnetic resonance curve corresponds to an effective storage time of ~ 1 second. The large dispersion of the UCN transit time through the Ramsey-type oscillating fields causes significant broadening of the resonance line width. The sensitivity of this experiment turned out to be $\sim 2 \times 10^{-22} e \cdot \text{cm}$ per day and was not competitive.

Several significant improvements were subsequently introduced leading to the first competitive result from the PNPI group [31]. First, a beryllium converter cooled to 30°K resulted in a 10 - 12 fold increase of the UCN flux. Second, an adiabatic method using

inhomogeneous magnetic field was implemented to rotate the neutron spin by 90° . This solved the dispersion problem encountered in the Ramsey method and the effective storage time was increased to 5 seconds. Third, a “differential double-chamber” spectrometer replaces the original single-chamber spectrometer. A common magnetic field was applied to the two adjacent identical chambers, while the applied electric fields in the two chambers have opposite signs. Upon reversal of the polarity of the electric field, the resonance frequency shift due to the neutron EDM, would be opposite in sign for the upper and lower chambers. In contrast, fluctuation of the common magnetic field will cause similar frequency shifts in both chambers. This enabled one to reduce the effect of the magnetic field instability. Finally, neutrons of opposite polarization direction were analyzed at the exit of each chamber with two separate detectors simultaneously. This allowed a two-fold increase in the count rates and also provided useful checks on systematic effects.

In the 1980 paper of the PNPI group [31], the UCN flux at the spectrometer input was $\sim 1.2 \times 10^4$ neutrons per second. A constant magnetic field of 28 mG and an electric field of ~ 25 kV/cm were applied to the double-chamber of ~ 20 liters each. The uniformity of the magnetic field within the chambers is within $(1-2) \times 10^{-5}$ Gauss. To achieve magnetic field stability, a passive three-layer magnetic shield provided a shielding factor of 10^3 . An active system consisting of a flux-gate magnetometer and Helmholtz coils was used to compensate and stabilize the external magnetic field. Another active system for stabilizing the magnetic field inside the shields was realized with the aid of an optical-pumping quantum magnetometer. From six different sets of measurements, the mean square deviation of the results is consistent with the expected statistical error, suggesting that the systematic error is negligible. The result, $d_n = (0.4 \pm 0.75) \times 10^{-24}$ e·cm, implied $|d_n| < 1.6 \times 10^{-24}$ e·cm at 90% confidence level.

In 1981, the PNPI group reported a new measurement [32] of neutron EDM. The major improvements included a new source of UCN based on a 150-cm^3 liquid hydrogen moderator [33] and a new coating for the chambers allowing total internal reflection for more energetic UCNs. The UCN intensity at the output of the spectrometer was improved by a factor of 7 to 8. From four different sets of measurements, they obtained [32], $d_n = (2.3 \pm 2.3) \times 10^{-25}$ e·cm. At 90% confidence level, $|d_n| < 6 \times 10^{-25}$ e·cm. In 1984, an updated result of $d_n = -(2 \pm 1) \times 10^{-25}$ e·cm was reported by Lobashev and Serebrov [34]. This implied $|d_n| < 4 \times 10^{-25}$ e·cm at 95% confidence level.

Major modifications for the PNPI experiment were reported [35] in 1986. In previous PNPI experiments, UCNs flowed continuously through the magnetic resonance

spectrometer with an average transit time of ~ 5 seconds. At this time the ILL stored UCN experiment [36] reported a confinement time of ~ 60 seconds. The PNPI group modified their spectrometer to allow prolonged confinement of the UCNs. They achieved a confinement time of ~ 50 seconds. A new universal source of cold and ultracold neutrons [37] was also used which provided a 3–4 times increase in UCN flux. The longer confinement time put more stringent requirement on the stability of the magnetic field, and two cesium magnetometers were positioned near the chambers for active stabilization of the magnetic field inside the spectrometer. The result of this experiment was $d_n = -(1.4 \pm 0.6) \times 10^{-25} e\cdot\text{cm}$, implying $|d_n| < 2.6 \times 10^{-25} e\cdot\text{cm}$ at 95% confidence level.

The most recent PNPI measurement was reported in 1992 [38], and a detailed account of this experiment was presented in a later paper [39]. The experimental setup was essentially the same as before [35], with minor modifications such as adding the fourth layer of the magnetic shield and adding the third cesium magnetometer near the chambers. The experiment consisted of 15 runs comprising a total of 13,863 measurement cycles. Each measurement cycle included filling the chambers with polarized UCN (30–40 s), confinement (70–100 s), and discharge and counting (40 s). A 2-second-long oscillating field pulse was applied at the beginning and at the end of the confinement time. The intensity of the uniform magnetic field was 18 mG, and the mean electric field was 14.4 kV/cm.

The result based on the analysis of the yields in the four neutron counters was $d_n = (0.7 \pm 4.0) \times 10^{-26} e\cdot\text{cm}$. From the analysis of the readings of the upper and lower magnetometers, a non-zero false EDM was found. Note that there should be no false EDM if the magnetometers faithfully measured the effective mean magnetic fields in the chambers. This false EDM was attributed to inhomogeneous magnetic pick-ups of various origins, including possible magnetization of the magnetic shield by sparks and spurious magnetic field generated by neighboring experimental apparatus affected by the reversal of the electric field. No correlation between d_n and the leakage current was found, showing that the leakage current was not a main source of the systematic effect. The amount of false EDM registered by the magnetometers suggested that a systematic correction of $-(1.9 \pm 1.6) \times 10^{-26} e\cdot\text{cm}$ needs to be applied to the measured EDM value. Therefore, the final result was

$$d_n = [2.6 \pm 4.0(\text{stat}) \pm 1.6(\text{syst})] \times 10^{-26} e \cdot \text{cm} . \quad (\text{III.13})$$

This result was interpreted as $|d_n| < 1.1 \times 10^{-25} e\cdot\text{cm}$ at 95% confidence level. Systematic errors appeared to limit the sensitivity of this experiment to few $10^{-26} e\cdot\text{cm}$.

C.2) UCN Measurements at ILL

Following the completion of the neutron EDM measurement [28] using the neutron beam magnetic resonance method, the interest at ILL shifted to the use of UCN [40], which would bypass the limitation imposed by the $\vec{v} \times \vec{E}$ effect. Unlike the PNPI group, the ILL group started out with the UCN storage bottle technique and did not use the less sensitive flow-through technique. The first ILL result was published in 1984 [36], which demonstrated the feasibility of measuring neutron EDM with stored UCN. A 5-liter cylindrical chamber contained polarized UCN of a density up to 0.05 per cm^3 , and neutrons precessed for 60 seconds in a uniform magnetic field of 10 mG and an electric field of 10 kV/cm. In contrast to the PNPI experiment, only one UCN storage chamber was implemented. Moreover, only a single detector was used to determine the number of neutrons having opposite polarization directions at the end of each storage cycle. From data collected in 136 one-day runs, a result of $d_n = (0.3 \pm 4.8) \times 10^{-25} e\cdot\text{cm}$ was obtained. Only statistical error was included, since the readings from three rubidium magnetometers showed negligible systematic effect.

The sensitivity of the ILL measurement was significantly improved in a subsequent experiment reported in 1990 [41]. A new neutron turbine [42] increased the UCN flux by a factor of 200 and a density of 10 UCN per cm^3 was achieved in the neutron bottle. The electric field was raised to 16 kV/cm and the leakage current was reduced from 50 nA to 5 nA. Following a three-year running period over 15 reactor cycles, the weighted average of these 15 data sets was $d_n = -(1.9 \pm 2.2) \times 10^{-26} e\cdot\text{cm}$, with a rather poor χ^2 per degree of freedom of 3.1. At this level of statistical accuracy, the difficulty of monitoring the magnetic field in the neutron bottle by the rubidium magnetometers, which were no closer than 40 cm to the axis of the bottle, became a dominant source of systematic error. After taking this uncertainty into account, the final result was reported to be $d_n = -(3 \pm 5) \times 10^{-26} e\cdot\text{cm}$, implying $|d_n| < 1.2 \times 10^{-25} e\cdot\text{cm}$ at the 95% confidence level.

To overcome the systematic uncertainty caused by magnetic field fluctuations in the UCN bottle, Ramsey suggested [43] the use of comagnetometers for EDM experiments. The idea was to store polarized atoms simultaneously in the same bottle as the neutrons. Fluctuation of the magnetic field will affect the spin precession of the comagnetometer atoms, which can be monitored. The ILL collaboration selected ^{199}Hg as the

comagnetometer. Effects from the ^{199}Hg EDM are negligible, since earlier experiments [44–46] showed that the EDM of ^{199}Hg was less than $8.7 \times 10^{-28} e\cdot\text{cm}$.

The most recent ILL experiment [47] used a 20-liter UCN bottle containing $3 \times 10^{10}/\text{cm}^3$ polarized ^{199}Hg . The UCN precession time was 130 seconds, roughly a factor of two improvement over previous experiment. However, the maximum electric field in this UCN bottle is only 4.5 kV/cm, roughly a factor of 3.5 lower than before. The UCN flux also appeared to be a factor of four lower than in the earlier experiment. Data were collected over ten reactor cycles of 50 days' length, and the ^{199}Hg comagnetometer was shown to reduce effects from magnetic field fluctuations significantly. The result of this experiment was $d_n = (1.9 \pm 5.4) \times 10^{-26} e\cdot\text{cm}$. A much improved χ^2 per degree of freedom of 0.97 was obtained for 322 measurement runs, and this was interpreted as an evidence for negligible systematic effects. An upper limit on the neutron EDM of $|d_n| < 9.4 \times 10^{-26} e\cdot\text{cm}$ was obtained at the 90% confidence level. When this result was combined with the result from the earlier ILL experiment [41], an improved upper limit of $6.3 \times 10^{-26} e\cdot\text{cm}$ was obtained. However, the method used to combine these two results was recently criticized by Lamoreaux and Golub [48], who argued that the two measurements should be treated independently.

The ILL experiment demonstrated the advantage of using a comagnetometer for reducing a dominant source of systematic error. It is conceivable that the sensitivity to the neutron EDM can be improved to a level better than $10^{-27} e\cdot\text{cm}$, provided that a more intense UCN flux together with a suitable comagnetometer, become available. In this proposal, we present a new approach for accomplishing this goal.

References

- [1] E. M. Purcell and N. F. Ramsey, *Phys. Rev.* **78**, 807 (1950).
- [2] J. H. Smith, Ph.D. thesis, Harvard University, 1951 (unpublished).
- [3] J. H. Smith, E. M. Purcell, and N. F. Ramsey, *Phys. Rev.* **108**, 120 (1957).
- [4] T. D. Lee and C. N. Yang, *Phys. Rev.* **104**, 254 (1956).
- [5] N. F. Ramsey, *Molecular Beams* (Oxford University Press, Oxford, 1956).
- [6] C. S. Wu, E. Ambler, R. Hayward, D. Hoppes, and R. Hudson, *Phys. Rev.* **105**, 1413 (1957).
- [7] R. Garwin, L. Lederman, and M. Weinrich, *Phys. Rev.* **105**, 1415 (1957).
- [8] J. Friedman and V. Telegdi, *Phys. Rev.* **105**, 1681 (1957).
- [9] L. Landau, *Nucl. Phys.* **3**, 127 (1957).
- [10] Ia. B. Zel'dovich, *J. Exp. Theor. Phys.* **6**, 1488 (1957) [*Sov. Phys. JETP* **6**, 1148 (1957)].
- [10a] N. F. Ramsey, *Phys. Rev.* **109**, 222 (1958).

- [11] J. Schwinger, *Phys. Rev.* **82**, 914 (1951); **91**, 713 (1953).
- [12] G. Lüders, *Kgl. Danske Videnskab Selskab. Mat. Fiz. Medd.* **28**, No 5 (1954); G. Lüders and B. Zumino, *Phys. Rev.* **106**, 385 (1957).
- [13] W. Pauli, in *Niels Bohr and the Development of Physics* (McGraw-Hill, New York, 1955).
- [14] J. H. Christenson, J. W. Cronin, V. L. Fitch, and R. Turlay, *Phys. Rev. Lett.* **13**, 138 (1964).
- [15] W. W. Havens, I. I. Rabi, and L. J. Rainwater, *Phys. Rev.* **72**, 634 (1947).
- [16] E. Fermi and L. Marshall, *Phys. Rev.* **72**, 1139 (1947).
- [17] C. G. Shull and R. Nathans, *Phys. Rev. Lett.* **19**, 384 (1967).
- [18] Yu. A. Alexandrov et al., *Yad. Fiz.*, **10**, 328 (1968).
- [19] C. G. Shull, *Phys. Rev. Lett.* **21**, 1585 (1968).
- [20] L. W. Alvarez and F. Bloch, *Phys. Rev.* **57**, 111 (1940).
- [21] N. F. Ramsey, *Phys. Rev.* **76**, 996 (1949); *Phys. Rev.* **84**, 506 (1951).
- [22] P. D. Miller, W. B. Dress, J. K. Baird, and N. F. Ramsey, *Phys. Rev. Lett.* **19**, 381 (1967).
- [23] W. B. Dress, J. K. Baird, P. D. Miller, and N. F. Ramsey, *Phys. Rev.* **170**, 1200 (1968).
- [24] J. K. Baird, P. D. Miller, W. B. Dress, and N. F. Ramsey, *Phys. Rev.* **179**, 1285 (1969).
- [25] W. B. Dress, P. D. Miller, and N. F. Ramsey, *Phys. Rev.* **D7**, 3147 (1973).
- [26] V. W. Cohen et al., *Phys. Rev.* **177**, 1942 (1969).
- [27] S. Apostolescu et al., *Rev. Roum. Phys.* **15**, 343 (1970).
- [28] W. B. Dress et al., *Phys. Rev.* **D15**, 9 (1977).
- [29] F. L. Shapiro, *Usp. Fiz. Nauk.* **95**, 145 (1968).
- [30] A. I. Egorov et al., *Yad. Fiz.* **21**, 292 (1975).
- [31] I. S. Altarev et al., *Nucl. Phys.* **A341**, 269 (1980).
- [32] I. S. Altarev et al., *Phys. Lett.* **102B**, 13 (1981).
- [33] I. S. Altarev et al., *Phys. Lett.* **A80**, 413 (1980).
- [34] V. M. Lobashev and A. P. Serebrov, *J. Phys. (Paris)* **45**, 3 (1984).
- [35] I. S. Altarev et al., *JETP Lett.* **44**, 460 (1986).
- [36] J. M. Pendlebury et al., *Phys. Lett.* **136B**, 327 (1984).
- [37] I. S. Altarev et al., *JETP Lett.* **44**, 345 (1986).
- [38] I. S. Altarev et al., *Phys. Lett.* **276B**, 242 (1992).
- [39] I. S. Altarev et al., *Phys. Atomic Nucl.* **59**, 1152 (1996).
- [40] R. Golub and J. M. Pendlebury, *Rep. Prog. Phys.* **42**, 439 (1979).
- [41] K. F. Smith et al., *Phys. Lett.* **234B**, 191 (1990).
- [42] A. Steyerl et al., *Phys. Lett.* **A116**, 347 (1987).
- [43] N. F. Ramsey, *Acta Phys. Hung.* **55**, 117 (1984).
- [44] S. K. Lamoreaux et al., *Phys. Rev. Lett.* **59**, 2275 (1987).
- [45] J. P. Jacobs et al., *Phys. Rev. Lett.* **71**, 3782 (1993).
- [46] J. P. Jacobs et al., *Phys. Rev.* **A52**, 3521 (1995).
- [47] P. G. Harris et al., *Phys. Rev. Lett.* **82**, 904 (1999).

[48] S. K. Lamoreaux and R. Golub, *Phys. Rev.* **D61**, 051301 (2000).